Journal of
Molluscan Studies

The Malacological Society of London

Journal of Molluscan Studies (2017) **83**: 476–480. doi:10.1093/mollus/eyx033
Advance Access publication date: 22 August 2017

RESEARCH NOTE

First record of carotenoid pigments and indications of unusual shell structure in chiton valves

B. A. Peebles[1], K. C. Gordon[2], A. M. Smith[1] and G. P. S. Smith[2]

[1]*Department of Marine Science, University of Otago, P.O. Box 56, Dunedin 9054, New Zealand; and*
[2]*Department of Chemistry, University of Otago, P.O. Box 56, Dunedin 9054, New Zealand*

Correspondence: B. A. Peebles; e-mail: bryce.peebles@gmail.com

Mollusc shells are typically made of calcite, aragonite or, in rare cases, vaterite (Weiner *et al.*, 2009; Ehrlich, 2010). These minerals are interspersed with protein matrix and sometimes pigments (Comfort, 1949a; Hedegaard, Bardeau & Chateigner, 2006). Typically, the organic matrix is composed of β-chitin, silk-like proteins rich in alanine and glycine, and aspartic acid-rich proteins (Weiner & Traub, 1984; Addadi *et al.*, 2006; Furuhashi *et al.*, 2010). This matrix creates an environment isolated from the surrounding seawater that the mollusc can supersaturate with calcium carbonate. Mineral layers of the shell develop by the nucleation of crystals of calcium carbonate within the protein matrix (Weiner & Traub, 1984). The proteins of the organic matrices of bivalve and gastropod shells have been the most intensively studied. It has been shown that these proteins determine the growth of specific crystal polymorphs of calcium carbonate (Marin & Luquet, 2004; Furuhashi *et al.*, 2010; Marin, Roy & Marie, 2012; Suzuki & Nagasawa, 2013).

Pigments found within the shell are typically melanins and tetrapyrroles, specifically porphyrins and bilins (Comfort, 1949a, b, c; Nicholas & Comfort, 1949; Gysi, Chapman & Moshier, 1979; Cai *et al.*, 2011). Comfort (1949b) identified porphyrins by observing their specific fluorescence in over 3,000 mollusc species. He also identified porphyrins using talc-adsorption chromatography in four pterioid bivalves, two caenogastropods and two vetigastropods (Comfort, 1949a). Nicholas & Comfort (1949) confirmed the presence of uroporphyrin in several mollusc shells using this method. In addition, Comfort (1949c) noted an unusual biliprotein initially suspected to be an indigoid. Cai *et al.* (2011) demonstrated a blue polyene in the shell of *Haliotis discus* by using a combination of UV-vis, infrared, NMR and ESI-mass spectroscopy. Using thin-layer chromatography and electrophoresis, Gysi *et al.* (1979) identified the pigments of *Haliotis californiensis* as bilipeptides.

Raman spectroscopy can also be used to identify molluscan shell pigments. Raman spectroscopy is a nondestructive analytical technique that uses lasers to identify compounds present within an unknown sample. Raman microscopy combines Raman spectroscopy with optical microscopy, thus allowing Raman spectra to be obtained from precise locations within a sample. Using Raman spectroscopy, coloured pigments in a wide range of gastropods, bivalves and *Nautilus* have been demonstrated to be polyenes (Thompson *et al.*, 2014), or specifically carotenoid polyenes (Barnard & de Waal, 2006; Hedegaard *et al.*, 2006). The characteristics of Raman spectra are determined by the specific chemical bonds present in the analysed material. While the technique cannot conclusively identify the compounds present, identification is attempted by comparison of spectra with known standards.

As in the case of shell proteins, work on shell pigments has focused on bivalves and gastropods. Reports on shell pigments from other classes of Mollusca are few (Matsuno, 2001; Barnard & de Waal, 2006; Hedegaard *et al.*, 2006; Karampelas *et al.*, 2009; Thompson *et al.*, 2014) and entirely lacking for the clade Aculifera (Polyplacophora and Aplacophora; Kocot *et al.*, 2011; Kocot, 2013). This lack is surprising in the case of chitons, which are common in the intertidal zone worldwide and include some species with a wide range of colour variation (Sigwart, 2016).

Chitons have a shell structure that differs from that of other molluscs. The shell of a chiton is composed of eight overlapping aragonitic plates, or valves. Each valve has an outer organic layer (properiostracum) covering the shell and two primary mineral layers, the outer (dorsal) tegmentum and the inner (ventral) articulamentum. The articulamentum forms the bulk of the valve and is a composite prismatic layer (Connors *et al.*, 2012). The dorsal tegmentum is also a prismatic layer which, uniquely in molluscan shells, incorporates sensory structures called aesthetes (Schwabe, 2010; Connors *et al.*, 2012). These are composed of a canal system, with large and small surface pores (megalaesthetes and micraesthetes, respectively; Schwabe, 2010). *Acanthopleura granulata* also incorporates eye-like structures into the tegmentum that may have the ability to form rudimentary images and in which the pigment pheomelanin has been identified (Speiser *et al.*, 2011; Li *et al.*, 2015). In addition, pigments in the tissues of six chiton species from Japan have been shown to include 27 different carotenoids, although the extracellular pigments within the mineralized layers of chiton valves, or in girdle spicules, have not yet been studied (Tsushima, Maoka & Matsuno, 1989; Schwabe, 2010; Maoka, 2011; Speiser, Demartini & Oakley, 2014; Sigwart, 2016).

Carotenoids were identified using Raman spectroscopy within the valves of eight chitons from New Zealand: *Acanthochitona zelandica*, *Chiton glaucus*, *Ischnochiton maorianus*, *Leptochiton inquinatus*, *Notoplax violacea*, *Onithochiton neglectus*, *Sypharochiton pelliserpentis* and *S. sinclairi*. Chitons were collected from the Otago Peninsula, South Island, New Zealand. At least three individuals of each of the eight species were collected and killed in 75% ethanol immediately after collection. The valves were dissected post-mortem and the soft tissues

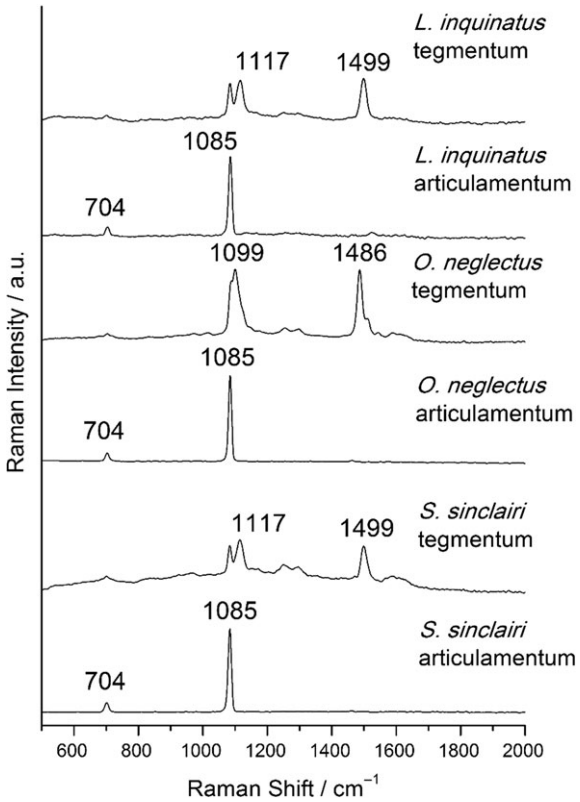

Figure 1. Raman spectra from the tegmentum and articulamentum of *Leptochiton inquinatus*, *Onithochiton neglectus* and *Sypharochiton sinclairi*. Bands at 704 and 1085 cm^{-1} indicate aragonite, peaks at 1099–1117 and 1486–1499 cm^{-1} indicate C=C and C–C bonds of carotenoids. Raman intensity is measured in arbitrary units (au).

Table 1. Stretching modes indicating presence of carotenoid pigments in chiton valves; υ^1 can be attributed to C=C; υ^2 can be attributed to C–C.

Species	υ_1 (cm^{-1})	υ_2 (cm^{-1})
Acanthochitona zelandica	1501	1118
Chiton glaucus	1506	1122
Ischnochiton maorianus	1500, 1513	1116, 1126
Leptochiton inquinatus	1499	1117
Notoplax violacea	1498	1115
Onithochiton neglectus	1486, 1510	1099, 1122
Sypharochiton pelliserpentis	1498, 1510	1116, 1122
Sypharochiton sinclairi	1499, 1510	1117, 1122

removed. The isolated valves were soaked overnight in a 0.5 M bleach solution to remove the properiostracum and any algal contaminants. The valves were then embedded in epoxy resin and warmed at 60°C for 2 h to harden. The resin block was cut with a diamond saw to section the valves. The exposed valve material was polished with a series of sandpapers (240 grit, 600 grit, then 1200 grit) followed by polishing on a Kent 3 automatic lapping machine with grit sizes of 3 µm then 1 µm. The polished valve sections were examined using a Senterra confocal Raman microscope (Bruker Optics, Ettlingen, Germany). The parameters used for Raman microscopy were: laser wavelength 785 nm, 100 mW laser power, 50 µm pinhole aperture, 20× objective, scan time 5 s with six co-additions and a spectral resolution of 9–18 cm^{-1}. Three line maps (each containing 20 spectra) were taken vertically through each valve, taking care to avoid the aesthete channels so that signals were strictly from the mineral layers. For each chiton species, line maps were obtained from each of the valves (I–VIII) for one of the three individuals and, from the head (I), fourth (IV) and tail (VIII) valves for the remaining two individuals. The Raman microscope was calibrated daily using a polystyrene standard.

The Raman spectra from complete valves showed prominent Raman bands at 704 cm^{-1} (aragonite), 1085 cm^{-1} (calcium carbonate), 1099–1126 cm^{-1} (C–C bond stretching) and 1498–1513 cm^{-1} (C=C bond stretching). The pigment signals were of the same relative strength as the calcium carbonate signal at 1085 cm^{-1}. The aragonite signal at 704 cm^{-1} was the smallest of the prominent peaks (Fig. 1). Aragonite signals were present in all spectra from all valves. The Raman bands at 1099–1126 and 1486–1513 cm^{-1} appeared only in the tegmentum; these bands are consistent with other Raman studies of molluscan shell pigments that have suggested carotenoids, based on peaks within the ranges 1070–1210 and 1450–1680 cm^{-1} (Britton *et al.*, 1997; Barnard & de Waal, 2006; Hedegaard *et al.*, 2006) (Fig. 1, Table 1). The occurrence of these putative carotenoids can be further refined by closer examination of the spectra. A green pigment was found in all analysed chiton valves with signals between 1486–1500 and 1099–1122 cm^{-1}. *Onithochiton neglectus*, *S. pelliserpentis*, *S. sinclairi* and *I. maorianus* (Chitonina) had an additional brown pigment in their tegmenta with signals at 1510–1513 and 1122–1126 cm^{-1}. The sole lepidopleuridan, *L. inquinatus*, the acanthochitonids (*A. zelandica* and *N. violacea*) and *C. glaucus* only contained the green pigment. The pigment signals detected in *L. inquinatus* were generally weaker than those found in the other chitons. Pigment signals detected from each species only varied by at most 8 cm^{-1}, except for those found in *O. neglectus*, which were shifted by at least 12 cm^{-1}. The Raman spectra of the chitons did not show features at 1400 or 1588 cm^{-1}, suggesting that eumelanin was not present at high concentrations within the valves (Huang *et al.*, 2004; Capozzi *et al.*, 2005; Coccato *et al.*, 2015; Perna, Lasalvia & Capozzi, 2016).

These green and brown carotenoids found in the tegmentum of chitons are the first instances of carotenoids reported in chiton skeletal material. Tsushima *et al.* (1989) have previously identified carotenoids within the tissue of *Liolophura japonica*, *Placiphorella japonica*, *P. stimpsoni*, *Acanthochitona defilippii*, *A. rebrolineata* and *Cryptochiton stelleri*, but did not analyse the valves or spicules of these species. Pigment signals in *L. inquinatus* (order Lepidopleurida) were weaker than those of the other seven species examined and the brown pigment was restricted to four members of the order Chitonida. Despite this apparent correlation between pigments and phylogeny, the presence of carotenoids could also be linked with the environment of the chitons. Since carotenoids can only be synthesized by plants (Barnard & de Waal, 2006), it is likely that the chitons incorporate pigments from their diet of intertidal algae. Dietary differences could explain the results for *O. neglectus*, which was found on kelp holdfasts rather than on rock as with the other sampled chitons. It is unlikely that these pigment signatures reported here are from algae living on or in the chiton valves, since in our data there were no cellular or non-pigment signals from algae (such as adhesion proteins, haemoglobin, chlorophylls and carbohydrates, as previously associated with algae; Parab & Tomar, 2012).

Small Raman bands appeared at 832–835 cm^{-1} (C–N bond stretching), 1270–1291 cm^{-1} (amide III band stretching), 1534–1536 cm^{-1} (amide II band stretching) and 1618–1620 cm^{-1} (C=O bond stretching) and were consistent between and within each examined species. These are indicative of protein, which is most likely part of the protein matrix of the shell. These signals were smaller than both aragonite signals and were found primarily in the outer mineralized layer, the tegmentum (Fig. 1). Few or no protein signals were found in the articulamentum, which only showed the strong aragonite signals (Fig. 2).

Decalcification of chiton valves was attempted using 0.5 M EDTA in order to remove the dominant aragonite signals and

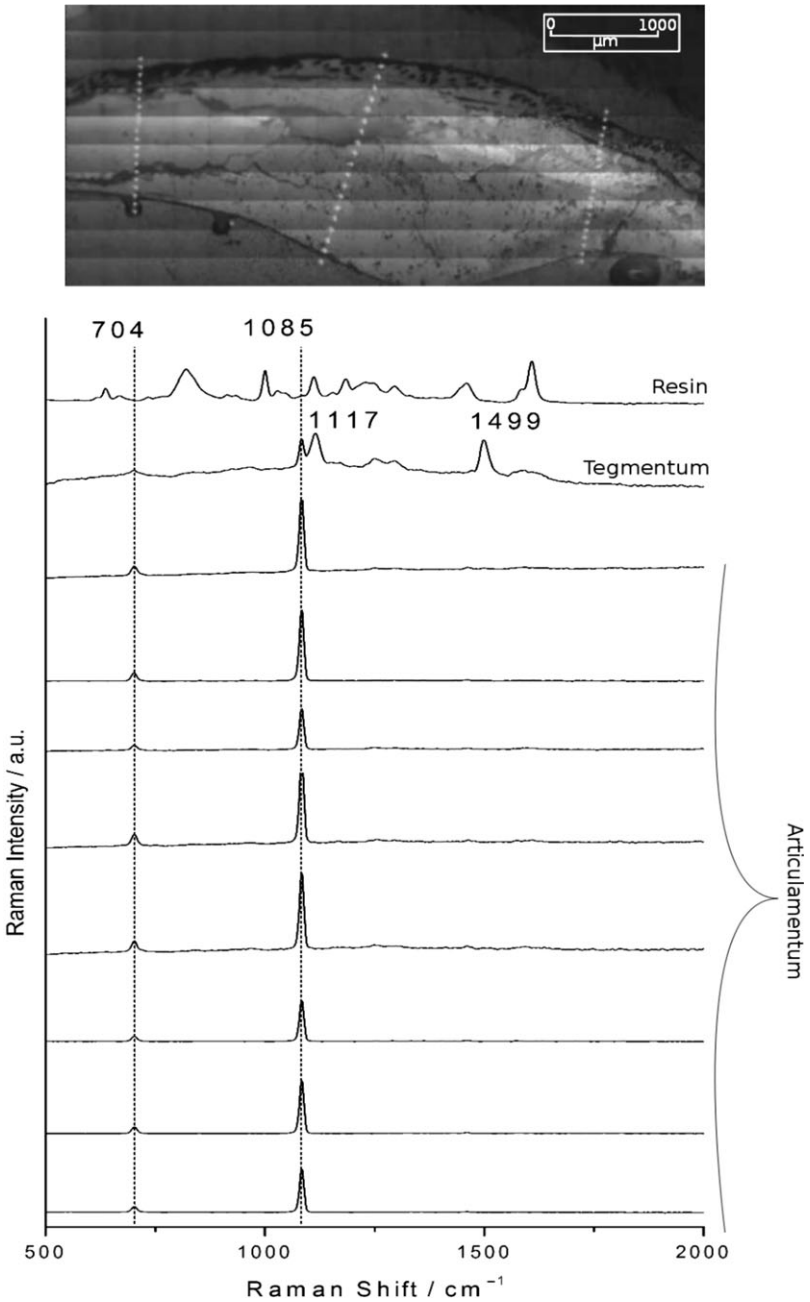

Figure 2. Raman bands from a representative line map across valve of *Sypharochiton sinclairi*. The lack of protein signals at 1110–1600 cm^{-1} from the tegmentum, and of pigment signals at 1117 and 1499 cm^{-1} from the articulamentum, were observed in all analysed species. The inset shows location of typical line maps on cross section of a valve; each grey dot is the location of a spectrum taken by the Raman microscope. Raman intensity is measured in arbitrary units (a.u.). Scale bar = 1 mm.

measure the isolated proteinaceous component of the chiton valves. This decalcification process resulted in the aragonite material dissolving, leaving a firm protein structure. Since the polysaccharides α-chitin and β-chitin have been described as major components of chiton valves, the decalcified valves should theoretically reveal the presence of chitin (Evans & Alvarez, 1999; Treves *et al.*, 2003; Weaver *et al.*, 2010; Connors *et al.*, 2012). However, while the decalcified valves showed stronger protein-related peaks in the same location as in the mineralized valves, and no aragonite signal, the spectra did not conclusively indicate the presence of chitin when compared with a chitin standard (Fig. 3; De Gelder *et al.*, 2007; Ehrlich *et al.*, 2007). The decalcified valves consistently showed peaks at 534, 930, 955, 1267 and 1621 cm^{-1}, whereas reference spectra from α-chitin showed peaks at 953–955, 1267 and 1621–1622 cm^{-1} (Fig. 3). The similarities indicate only that both the decalcified material and α-chitin have a C–C bond (955 cm^{-1}) and an amide group (1267 cm^{-1}). Notably, α-chitin also shows peaks at 1621 and 1656 cm^{-1} (Mikkelsen *et al.*, 1997), of which the decalcified valves show only the first, at 1621 cm^{-1}. The decalcified material also appears to be missing the characteristic chitin peaks at 1087, 1109, 1149, 1204, 1324, 1374, 1417 and 1450 cm^{-1} (Mikkelsen *et al.*, 1997). The match between the spectra of the decalcified valves and the α-chitin standard is not sufficiently close to identify chitin with confidence.

These are the first data to suggest an unusual composition of chiton shells among molluscs. In other mollusc shells each aragonite

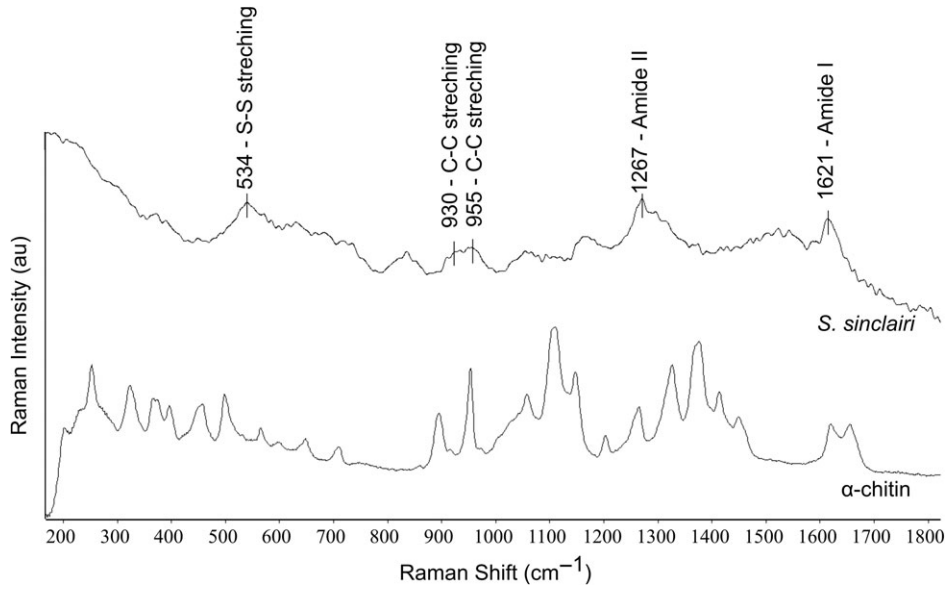

Figure 3. Raman spectra of a decalcified *Sypharochiton sinclairi* valve and of α-chitin. The major peaks of α-chitin do not appear in the spectrum from *S. sinclairi*. Raman intensity is measured in arbitrary units (au).

crystal is surrounded by an organic matrix of protein and chitin, which is integral to the process by which the shell is formed (Bøggild, 1930; Weiner & Traub, 1984; Addadi *et al.*, 2006). The absence of evidence of α-chitin and β-chitin in the chiton valves is therefore intriguing, especially since chitin has previously been reported in chitons. Treves *et al.* (2003), using IR spectroscopy, found that chitin was abundantly present in the valves of *Acanthopleura villantii*, although absent from its girdle spicules. Weaver *et al.* (2010) examined the radula of *C. stelleri* using both transmission electron microscopy and Raman spectroscopy and found α-chitin. FTIR spectroscopy has been used to detect α-chitin in the matrix component of valves and girdle spicules of *Tonicella marmorea* and in the radula of *S. pelliserpentis* (Evans & Alvarez, 1999; Connors *et al.*, 2012). These conflicting results should be examined by future studies using both Raman and IR microscopy. The lack of protein signals in the articulamentum is also unexpected, since the organic matrix used for calcification should be present throughout the valve. It is likely that matrix proteins were present in the articulamentum but below detection levels, since a solid material did remain when the valves were decalcified.

ACKNOWLEDGEMENTS

Thanks to Professor Hamish Spencer and Erin Bowkett for collecting chitons with us for this study. Many thanks to Brent Pooley for his support in sectioning, polishing and resin-embedding of samples. We acknowledge support from the Departments of Marine Science and Chemistry, University of Otago.

REFERENCES

ADDADI, L., JOESTER, D., NUDELMAN, F. & WEINER, S. 2006. Mollusc shell formation: a source of new concepts for understanding biomineralization processes. *Chemistry—A European Journal*, **12**: 980–987.

BARNARD, W. & DE WAAL, D. 2006. Raman investigation of pigmentary molecules in the molluscan biogenic matrix. *Journal of Raman Spectroscopy*, **37**: 342–352.

BØGGILD, O.B. 1930. The shell structure of the mollusks. *Kongelige Danske Videnskabernes Selskabs Skrifter Naturvidenskabelig og Mathematiske Afdeling*, **9**: 231–326.

BRITTON, G., WEESIE, R.J., ASKIN, D., WARBURTON, J.D., GALLARDO-GURRERO, L., JANSEN, F.J., DE GROOT, H.J.M., LUGTENBURG, J., CORNARD, J.P. & MERLIN, J.C. 1997. Carotenoid blues: structural studies on carotenoproteins. *Pure and Applied Chemistry*, **69**: 2075–2084.

CAI, Z., WU, J., CHEN, L., GUO, W., LI, J., WANG, J. & ZHANG, Q. 2011. Purification and characterisation of aquamarine blue pigment from the shells of abalone (*Haliotis discus hanni* Ino). *Food Chemistry*, **128**: 129–133.

CAPOZZI, V., PERNA, G., GALLONE, A., BIAGI, P.F., CARMONE, P., FRATELLO, A., GUIDA, G., ZANNA, P. & CICERO, R. 2005. Raman and optical spectroscopy of eumelanin films. *Journal of Molecular Structure*, **744–747**: 717–721.

COCCATO, A., JEHLICKA, J., MOENS, L. & VANDENABEELE, P. 2015. Raman spectroscopy for the investigation of carbon-based black pigments. *Journal of Raman Spectroscopy*, **46**: 1003–1015.

COMFORT, A. 1949a. Acid-soluble pigments of molluscan shells 2. Pigments other than porphyrins. *Biochemical Journal*, **45**: 199–204.

COMFORT, A. 1949b. Acid-soluble pigments of shells 1. The distribution of porphyrin fluorescence in molluscan shells. *Biochemical Journal*, **44**: 111–117.

COMFORT, A. 1949c. Acid-soluble pigments of molluscan shells 3. The indigoid character of the blue pigment of *Haliotis cracherodii* Leach. *Biochemical Journal*, **45**: 204–208.

CONNORS, M.J., EHRLICH, H., HOG, M., GODEFFROY, C., ARAYA, S., KALLAI, I., GAZIT, D., BOYCE, M. & ORTIZ, C. 2012. Three-dimensional structure of the shell plate assembly of the chiton *Tonicella marmorea* and its biomechanial consequences. *Journal of Structural Biology*, **177**: 314–328.

DE GELDER, J., DE GUSSEM, K., VANDENBEELE, P. & MOENS, L. 2007. Reference database of Raman spectra of biological molecules. *Journal of Raman Spectroscopy*, **38**: 1133–1147.

EHRLICH, H. 2010. Chitin and collagen as universal and alternative templates in biomineralization. *International Geology Review*, **52**: 661–699.

EHRLICH, H., MALDONADO, M., SPINDLER, K., ECKERT, C., HANKE, T., BORN, R., GOEBEL, C., SIMON, P., HEINEMANN, S. & WORCH, H. 2007. First evidence of chitin as a component of the skeletal fibers of marine sponges. Part I. Verongidae (Demospongia: Porifera). *Journal of Experimental Zoology Part B, Molecular and Developmental Evolution*, **308**: 347–356.

EVANS, L.A. & ALVAREZ, R. 1999. Characterization of the calcium biomineral in the radular teeth of *Chiton pelliserpentis*. *Journal of Biological Inorganic Chemistry*, **4**: 116–170.

FURUHASHI, T., MIKSIK, I., SMRZ, M., GERMANN, B., NEBIJA, D., LACHMANN, B. & NOE, C. 2010. Comparison of aragonitic molluscan shell proteins. *Comparative Biochemistry and Physiology Part B*, **155**: 195–200.

GYSI, J.R., CHAPMAN, D.J. & MOSHIER, S.E. 1979. Comparative biochemistry of *Haliotis* pigmentation: unusual bilipeptides of *Haliotis cracherodii*. *Comparative Biochemistry and Physiology*, **63B**: 355–361.

HEDEGAARD, C., BARDEAU, J.F. & CHATEIGNER, D. 2006. Molluscan shell pigments: an *in situ* resonance Raman study. *Journal of Molluscan Studies*, **72**: 157–162.

HUANG, Z., LUI, H., CHEN, X.K., ALAJLAN, A., MCLEAN, D.I. & ZENG, H. 2004. Raman spectroscopy of in vivo cutaneous melanin. *Journal of Biomedical Optics*, **9**: 1198–1205.

KARAMPELAS, S., FRITSCH, E., MEVELLEC, J.Y., SKLAVOUNOS, S. & SOLDATOS, T. 2009. Role of polyenes in the coloration of cultured freshwater pearls. *European Journal of Mineralogy*, **21**: 85–97.

KOCOT, K.M., CANNON, J.T., TODT, C., CITARELLA, M.R., KOHN, A.B., MEYER, A., SANTOS, S.R., SCHANDER, C., MOROZ, L.L., LIEB, B. & HALANYCH, K.M. 2011. Phylogenomics reveals deep molluscan relationships. *Nature*, **477**: 452–456.

KOCOT, K.M. 2013. Recent advances and unanswered questions in deep molluscan phylogenetics. *American Malacological Bulletin*, **31**: 195–208.

LI, L., CONNORS, M.J., KOLLE, M., ENGLAND, G.T., SPEISER, D.I., XIAO, X., AIZENBURG, J. & ORTIZ, C. 2015. Multifunctionality of chiton biomineralized armor with an integrated visual system. *Science*, **350**: 952–956.

MAOKA, T. 2011. Carotenoids in marine animals. *Marine Drugs*, **9**: 278–293.

MARIN, F. & LUQUET, G. 2004. Molluscan shell proteins. *Comptes Rendus Palevol*, **3**: 469–492.

MARIN, F., ROY, N. & MARIE, B. 2012. The formation and mineralization of mollusk shell. *Frontiers in Bioscience*, **4**: 1099–1125.

MATSUNO, T. 2001. Aquatic animal carotenoids. *Fisheries Science*, **67**: 771–783.

MIKKELSEN, A., ENGELSEN, S.B., HANSEN, H.C.B., LARSEN, O. & SKIBSTED, L.H. 1997. Calcium carbonate crystallization in the α-chitin matrix of the shell of pink shrimp, *Pandalus borealis*, during frozen storage. *Journal of Crystal Growth*, **177**: 125–134.

NICHOLAS, R.E.H. & COMFORT, A. 1949. Acid-soluble pigments of molluscan shells 4. Identification of shell porphyrins with particular reference to conchoporphyrin. *Biochemical Journal*, **45**: 208–210.

PARAB, N.D.T. & TOMAR, V. 2012. *R*aman spectroscopy of algae: a review. *Nanomedicine & Nanotechnology*, **3**(131): 1–7.

PERNA, G., LASALVIA, M. & CAPOZZI, V. 2016. Vibrational spectroscopy of synthetic and natural eumelanin. *Polymer International*, **65**: 1323–1330.

SCHWABE, E. 2010. Illustrated summary of chiton terminology. *Spixiana*, **33**: 171–194.

SIGWART, J.D. 2016. The chiton stripe tease. *Marine Biodiversity*, **46**: 1–2.

SPEISER, D.I., DEMARTINI, D.G. & OAKLEY, T.H. 2014. The shell-eyes of the chiton *Acanthopleura granulata* (Mollusca, Polyplacophora) use pheomelanin as a screening pigment. *Journal of Natural History*, **48**: 2899–2911.

SPEISER, D.I., EERNISSE, D.J. & JOHNSEN, S. 2011. A chiton uses aragonite lenses to form images. *Current Biology*, **21**: 665–670.

SUZUKI, M. & NAGASAWA, H. 2013. Mollusk shell structures and their formation mechanism. *Canadian Journal of Zoology*, **91**: 349–366.

THOMPSON, C.M., NORTH, E.W., WHITE, S.N. & GALLAGER, S. M. 2014. An analysis of bivalve larval shell pigments using micro-Raman spectroscopy. *Journal of Raman Spectroscopy*, **45**: 349–358.

TREVES, K., TRAUB, W., WEINER, S. & ADDADI, L. 2003. Aragonite formation in the chiton (Mollusca) girdle. *Helvetica Chimica Acta*, **86**: 1101–1112.

TSUSHIMA, M., MAOKA, T. & MATSUNO, T. 1989. Comparative biochemical studies of carotenoids in marine invertebrates—the first positive identification of ϵ,ϵ-carotene derivatives and isolation of two new carotenoids from chitons. *Comparative Biochemistry and Physiology Part B: Comparative Biochemistry*, **93**: 655–671.

WEAVER, J.C., WANG, Q., MISEREZ, A., TANTUCCIO, A., STROMBERG, R., BOZHILOV, K.N., MAXWELL, P., NAY, R., HEIER, S.T., DIMASI, E. & KISAILUS, D. 2010. Analysis of an ultra hard magnetic biomineral in chiton radular teeth. *Materials Today*, **13**: 42–52.

WEINER, S., MAHAMID, J., POLITI, Y., MA, Y. & ADDADI, L. 2009. Overview of the amorphous precursor phase strategy in biomineralization. *Frontiers of Materials Science in China*, **3**: 104–108.

WEINER, S. & TRAUB, W. 1984. Macromolecules in mollusc shells and their functions in biomineralization. *Philosophical Transactions of the Royal Society B: Biological Sciences*, **304**: 425–434.